

Author Version: *Sci. Total Environ.*: 566-567; 2016; 1052-1061

## **Effects of bottom water dissolved oxygen variability on copper and lead fractionation in the sediments across the oxygen minimum zone, Western Continental margin of India**

P. Chakraborty<sup>\*1</sup>, Sucharita Chakraborty<sup>1</sup>, Saranya Jayachandran<sup>1</sup>, Ritu Madan<sup>1</sup>, Arindam Sarkar<sup>1</sup>, Linsy P.<sup>1</sup>, B. Nagender Nath<sup>1</sup>

<sup>1</sup>Geological Oceanography Division, National Institute of Oceanography (CSIR), Dona Paula, Goa, 403004, India

### **Corresponding Author:**

Phone-91-8322450495; Fax: 91-832-2450602, E-mail: [pchak@nio.org](mailto:pchak@nio.org)

### **ABSTRACT:**

This study describes the effect of varying bottom-water oxygen concentration on geochemical fractionation (operational speciation) of Cu and Pb in the underneath sediments across the oxygen minimum zone (Arabian Sea) in the west coast of India. Both, Cu and Pb were redistributed among the different binding phases of the sediments with changing dissolved oxygen level (from oxic to hypoxic and close to suboxic) in the bottom water. The average lability of Cu-sediment complexes gradually decreased (i.e., stability increased) with the decreasing dissolved oxygen concentrations of the bottom water. Decreasing bottom-water oxygen concentration increased Cu association with sedimentary organic matter. However, Pb association with Fe(III)/Mn-oxyhydroxide phases in the sediments gradually decreased with the decreasing dissolved oxygen concentration of the overlying bottom water (due to dissolution of Fe (III)/Mn oxyhydroxide phase). The lability of Pb-sediment complexes increased with the decreasing bottom-water oxygen concentration. This study suggests that bottom-water oxygen concentration is one of the key factors governing stability and lability of Cu and Pb complexes in the underneath sediment. Sedimentary organic matter and Fe (III)/Mn oxyhydroxide binding phases were the major hosting phases for Cu and Pb respectively in the study area. Increasing lability of Pb- complexes in bottom sediments may lead to positive benthic fluxes of Pb at low oxygen environment.

**Keywords:** Oxygen minimum zone; redox and metal speciation; Cu-speciation; Pb-speciation; OMZ Arabian Sea

## INTRODUCTION

Changes in concentrations of dissolved oxygen in overlying bottom water can modify metals speciation in the bottom sediments (Calmano et al., 1993; Middleburg and Levin, 2009). Different fractions of metals (operational speciation) in sediment can be classified based upon their association with different binding phases in the sediments: acid soluble forms (water soluble, exchangeable and carbonate/bicarbonate forms); reducible forms (metal associates with Fe, Mn-oxyhydroxide binding phases); oxidizable forms (metal associates with sedimentary organic carbon binding phases); and residual forms (metal within the structure of sediment). The first three forms of metals (acid soluble, reducible and oxidizable) are considered as bioavailable forms of metals (non-residual) in sediment. The residual fraction of metal is considered as inert and non-bioavailable pool (Alvarez et al., 2002; Kwon, and Lee, 2001; Chakraborty et al., 2012; 2014) of metals.

Sedimentary organic matter and Fe/Mn oxyhydroxide have been reported to be the major metal binding phases in oxic sediments (Luoma and Bryan 1981; Tack and Verloo, 1995). Reduction of Fe (III), and Mn(IV) (from Fe/Mn-oxyhydroxide) predominates under hypoxic or anoxic condition (Greatz et al, 1973). However, preservation of sedimentary organic matter has been reported under the same condition (Jahnke et al., 1982; Henrichs and Reeburgh 1987; Lovely, 1987; Pedersen and Calvert, 1990). Thus, a change in dissolved oxygen concentration (from oxic to hypoxic and then close to suboxic) in overlying water can modify Fe (III)/Mn-oxyhydroxide and sedimentary organic binding phases of the bottom sediments. It has been reported that hypoxic condition of overlying water causes release of dissolved Fe(II) and Mn(II) from Fe/Mn oxyhydroxide phase of the sediment and preserve organic matter in the sediment (Middleburg and Levin, 2009). Thus, changes in bottom water oxygen levels may alter the distribution and speciation of metals associated with these two major metal binding phases.

Copper (Cu) has been reported to have significant affinity towards organic phases in marine sediments (Chakraborty et al., 2015a; Chakraborty et al., 2016; Flemming and Trevors, 1989; Hanson and Quinn 1983). Major fractions of non-residual Cu has been reported to associate with sedimentary organic matter (oxidizable form). However, lead (Pb) has been reported to show strongest affinity for Fe/Mn-oxyhydroxide phase in sediments (reducible phase) (Chakraborty et al., 2015a; Chakraborty et al., 2015b; Belzile et al., 1989). Thus, distinct effects of varying bottom water oxygen concentration are expected to impact Cu and Pb speciation (as Fe/Mn-oxyhydroxide and sedimentary organic matter are the major hosting phases for these two metals) in the bottom sediments.

The Arabian Sea hosts the second-most intense perennial oxygen minimum zone (OMZ) in the world tropical ocean (Kamykowski and Zentara, 1990), with near-total depletion of oxygen at depths from 150 to 1000 m (Banse et al., 2014; Morrison et al., 1998). It is of global biogeochemical significance because of denitrification in the upper part leading to N<sub>2</sub> and N<sub>2</sub>O production (Naqvi and Noronha, 1991). The residence time of OMZ water is believed to be less than a decade (Banse et al., 2014). The upper few hundred meters of this zone has been reported to be nearly anoxic but non-sulfidic (Banse et al. 2014). Naqvi and Noronha (1991) have also reported that this zone is predominantly suboxic ( $\leq 5 \mu\text{mol O}_2/\text{kg}$ ) in nature. The changing redox condition of overlying bottom water from this region is expected to have tremendous impact on Cu and Pb speciation in the bottom sediments across the OMZ, and thus, this study was undertaken, across the two transects of the OMZ in the eastern Arabian Sea.

The aim of this study was to investigate (for the first time) the impact of changing bottom water oxygen concentration on geochemical fractionation of Cu and Pb complexes and their stability in the bottom sediment.

## **Materials and methods:**

### **Description of study sites**

Sediment samples were collected in two transects passing through the perennial OMZ from the western continental margin of India. The semi-annual reversal in wind stress associated with the monsoon, water mass intrusions from marginal seas and the other oceans, and no opening to the north with no subtropical convergence or deep water formation are some of the typical characteristics of the Arabian Sea, which leads to a unique thermohaline structure and circulation pattern (Morrison et al., 1999). It has been reported that upwelling-favourable conditions exist along the southern shelf (off Karwar), which is less conspicuous toward the northern part of the western continental margin (off Gujarat) of India (Muraleedharan and Kumar 1996). There is always a permanent pycnocline in this region. However, the top of the pycnocline depth changes with season and gives rise to seasonal pycnocline in this area (de Boyer et al., 2004; Prasanna Kumar et al., 2004; Shetye et al. 1994).

The sediment samples were collected on board ORV Sindhu Sankalp (SSK71 and SSK 80) during 8<sup>th</sup>-21<sup>st</sup> November 2014 and 26<sup>th</sup> -30<sup>th</sup> March 2015 along two transects from the western continental margin viz., off Karwar (SSK#80) and off Gujarat (SSK#71) across the perennial OMZ (**Figure 1a**). The sediment samples were collected from the outer shelves (Stations # SSK 71/SPC 15, SSK 71/SPC 16, SSK80/SPC2), the upper slopes (stations # SSK 71/SPC 17, SSK80/SPC4, SSK80/SPC5), the middle slopes (stations # SSK71/SPC18, SSK80/SPC6) and the deeper region of

the slopes (Stations # SSK 71/SPC 21, SSK80/SPC7) (as shown in **Figure 1b**). The bottom water samples were also collected at each station by using a CTD rosette fitted with Niskin bottles (Sea-Bird, USA). Dissolved oxygen concentrations in the overlying bottom seawater were determined by Winkler method. The detailed description of the method has been given in literature (Broenkow and Cline, 1969; Bryan et al., 1976). The pH of the water samples were determined by pH meter (LabIndia, Mumbai, India). CTD rosette (Sea-Bird, USA) was used to know the salinity of the overlying bottom water.

The sediment samples were collected in such a way to ensure that there were distinct variations in the dissolved oxygen (DO) concentration of the overlying bottom waters. The definitions of various stages of oxygen deficiency in seawater are described in **Table 1**. **Table 2** presents the details of the sediment sampling locations and the variation in, temperature salinity, dissolved oxygen concentration and redox state of the overlying bottom water. Spade corer of 30cm × 15cm × 50 cm was used to collect the sediment samples across the OMZ. The sediments cores were stored at -4°C and brought back to the laboratory. The surface sediments were sub-sampled from the short sediment cores under laboratory condition, freeze dried and stored (packed in air tight zip lock bag) at -4° C until required for analysis. The thickness of the surface layer of sediments was 0-1 cm. The colours of the surface sediments remained unchanged during their processing. This observation suggests that oxygenation of the sediment samples probably did not occur.

### **Sediment texture**

Texture of the dry sediment (in < 63µm) was analyzed by Particle Size Analyzer (LPSA from Malvern Mastersizer 2000, Worcestershire, UK.). The detailed procedure has been described in the literature by Ramaswamy and Rao (2006). The sand data is presented in weight percentage (wt %) and the silt and clay in vol (%) in this study.

### **Total inorganic carbon (TIC), total nitrogen (TN) and total sedimentary organic carbon (TOC)**

The surface sediment samples were analyzed for total carbon (TC), total inorganic carbon (TIC), and total nitrogen (TN) contents in the sediments. The TC and TN contents in sediments were determined using a Flash 2000 CHN elemental analyzer (Thermo Fisher Scientific Incorporation). The precision of the analysis was within ± 5%. The NC reference soil sample (containing 0.37% N and 3.5% C) was used as the certified reference material. TIC was determined by coulometry (UIC Coulometrics, Illinois, USA). Calcium carbonate (12% C) was used as a standard material. The relative standard deviation of the analysis was within ± 2%. The total organic carbon (OC) content was derived by

deducting TIC from TC.  $\text{CaCO}_3$  content in sediment was calculated assuming that the majority of inorganic carbon (or carbonate) is associated with Ca.

### **Sequential Extraction protocol**

The modification of BCR sequential extraction protocol proposed by Chakraborty et al. (2014a) was used in this study for geochemical fractionation of Cu and Pb in the sediments. In this modified protocol, an additional step of extraction of water soluble metal complexes (a good indicator of bioavailability) from the sediments was included. This step also helps to remove excess salt content from the marine sediments. Thus, the modified BCR protocol allows us to separate and determine the concentrations of water soluble metal complexes (Fr. 1); ion-exchangeable, and carbonate/bicarbonate forms of metals (Fr. 2); metals bound to Fe–Mn oxyhydroxides i.e., reducible fraction of metals (Fr. 3); concentrations of metals associated with organic phases, i.e., oxidizable fraction of metals (Fr. 4) and residual metal fraction (Fr. 5) in sediment.

All the extraction processes were performed in Teflon containers. The reagents used in this study were of suprapur grade or better (ultrapure). The protocol has been vividly described in literature (Chakraborty et al 2014a). The concentrations of both the metals in each extracted solution and in residual fraction were determined by electrothermal atomic absorption spectrometer (ETAAS). BCR-701 was used as certified sediment reference material (CRM) (produced by IRMM- Institute Reference material and Measurements, Geel, Belgium and marketed by Sigma Aldrich). The BCR-701 certificate does not provide certified values for the water soluble fraction. Thus, Fr1 and Fr.2 (determined by the modified method) were added and compared with the certified reported values. Validation of the sequential extraction method was also done by comparing the total metal concentrations (determined by ETAAS) with the sum of the concentrations of metal fractions obtained by following the modified sequential extraction protocols. The comparable (close to 100% recovery) values of total metal concentrations support the reliability and validity of the sequential extraction method. The recovery of certified Cu and Pb in different geochemical fraction from BCR-701 were very good and well within the acceptable range ( $\pm 3\%$  of the reported values in each fraction). Replicate extractions of three independent sub-samples were done. Three analytical measurements of each extractant were carried out. Less than 1 % was the RSD associated with the measurements ( $n=3$ ) for Cu and Pb.

### **Electrothermal Atomic Absorption Spectrometer (ETAAS)**

ETAAS (Perkin Elmer, PinAAcle 900T, Waltham, Massachusetts, USA) was used for the determination of the total metal concentrations in the sediments. This instrument was equipped with

an AS900 auto sampler. The transversely heated graphite tubes (Perkin-Elmer) were pyrolytically coated and were equipped with integrated L'vov platforms. During the drying, ashing and clean-up cycles, the internal argon gas was passed through the furnace at  $300 \text{ cm}^3 \text{ min}^{-1}$ , but the gas flow was interrupted during the atomization step. The instrumental parameters of drying temperature, ashing temperature and atomization temperature for Cu and Pb are presented in Table 3. A mixture  $5 \mu\text{L}$  of modifier (containing  $0.05 \text{ mg}$  of ammonium hydrogen phosphate ( $\text{NH}_4 \text{H}_2 \text{PO}_4$ ) and  $0.003 \text{ mg}$  of magnesium nitrate ( $\text{Mg}(\text{NO}_3)_2$ ) was added to  $15 \mu\text{L}$  of sample solution for Pb analysis (<http://www.cdc.gov/niosh/docs/2003-154/pdfs/7105.pdf>). The signal was measured in the peak area mode. Every fifth sample analysed was a blank. Replicate extractions of three independent sub-samples were done. All measurements were carried out in triplicate.

The total metals concentrations in the studied sediments were determined by digesting  $0.05 \text{ g}$  of sediments samples with  $10.0 \text{ cm}^3$  of acid mixtures of HF (Merck, Suprapur 40%,Darmstadt, Germany),  $\text{HNO}_3$  (Merck, Suprapur 65%,Darmstadt, Germany) and  $\text{HClO}_4$  (Fluka analytical 70%, Sigma Aldrich, Canada) (in 7:2:1 ratio) on a hot plate( $180^\circ\text{C}$ ). The sediments were digested and evaporated to dryness. The residues were re-dissolved in 2%  $\text{HNO}_3$  (Merck, Suprapur 65%, Darmstadt, Germany) and analyzed by ETAAS.

MAG-1, a fine grained gray-brown clayey mud with low carbonate content, from the Wilkinson Basin of the Gulf of Maine, was used as CRM (obtained from United States Geological Survey, Virginia, USA). The reported certified reference concentrations of Cu and Pb in MAG-1 were  $30.0 \pm 3.0 \text{ mg/kg}$  and  $24.0 \pm 3.0 \text{ mg/kg}$  respectively. The recovered concentrations of total Cu and Pb from MAG-1 were  $29.3 \pm 0.3 \text{ mg/kg}$  and  $23.9 \pm 0.3 \text{ mg/kg}$  respectively.

#### **Kinetic fractionation study:**

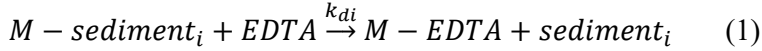
The lability and stability of metal complexes in the sediments was investigated by determining ethylenediaminetetraacetate (EDTA)-extractable trace metals concentrations (from the sediments) as a function of time. EDTA was chosen as the extracting reagent, as it is a well-characterized, strong chelating agent that allows good control of experimental variables. Most EDTA-metal chelate complexes are formed rapidly and are extremely stable (Welcher 1958). The use of EDTA as a complexing agent avoids difficulties associated with other complexants in that a single 1:1 complex species is formed rather than a stepwise formation of complexes, which helps to simplify calculations and interpretation of results (Welcher 1958). As a hexaprotic acid, it has an inherently large pH buffering capacity. In addition, it forms negatively charged metal complexes at most pH values, helping to keep extracted metals in solution by minimizing re-adsorption of extracted metals

to the sediment. The kinetic extraction procedure has been described in detail in the literature (Chakraborty et al 2012, Chakraborty, 2012). The kinetic extraction experiments were performed in triplicate for all the samples to ensure repeatability of results. Ethylenediaminetetraacetate (EDTA)-extractable Cu and Pb concentrations were determined directly by ETAAS.

### Theory of kinetic fractionation study

Kinetically distinguishable forms of metals in the sediments and their stability were studied by using kinetic model proposed by Olson and Shuman (1985). It is based on the assumption that each sediment sample consists of  $n$  different components, in which each component,  $M$ -sediment $_i$ , exists in equilibrium with its dissociation products:  $M^{2+}$  or extractable  $M$  complexes, and naturally occurring heterogeneous complexant, sediment $_i$ . The subscript,  $i$ , represents different binding sites of the naturally-occurring heterogeneous complexant.

The extraction of metals from sediment using EDTA (as an extractant) is represented by the following reactions (charges are omitted for simplicity):



Where  $M - sediment_i$  and  $M - EDTA$  represent the metal ion  $M$ , bound to a sediment binding site, sediment $_i$ , and EDTA, respectively. If EDTA is added in large excess, the  $M$  is extracted from the original sediment binding site with a rate constant  $k_i$ . The change in concentration of  $M - sediment_i$  with time is given by the following pseudo first-order rate law.

$$-\frac{dc_{M-sediment_i}}{dt} = k_{di}c_{M-sediment_i} \quad (2)$$

The integrated rate law derived from equation 2, expressed in terms of the concentration of  $M$ -EDTA, shows that the concentration of metal extracted in solution,  $c_{M-EDTA}$ , rises exponentially over time to a limiting value, as shown in Eq. 3. Unfortunately, it is impossible to study the individual binding sites separately, or to a priori know the number of discrete binding sites, and there may be a nearly continuous distribution of sediment binding sites. Hence, Eq. 3 is written as a summation of exponentials.

$$C_{M-EDTA}(t) = \sum_{i=1}^n C_{M-sediment_i}(1 - e^{-k_{di}t}) \quad (3)$$

This system described by equation 3 can be approximated by a two -component first-order reaction model.  $c_{M-EDTA}(t) = c_1(1 - e^{k_{d1}t}) + c_2(1 - e^{k_{d2}t})$  (4)

Where,  $c_{M-EDTA}(t)$  is the concentration of M (Cu or Pb) extracted by EDTA at time  $t$ ,  $c_1, c_2$  are the concentrations of EDTA-extractable M initially bound to labile (quickly extracted), or stable (with respect to the time scale of measurement) sediment binding sites, respectively, and  $k_{d1}, k_{d2}$  are the corresponding dissociation rate constants.

### Non-linear regression analysis for kinetic measurement

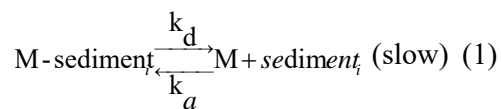
Analysis of experimental data to obtain physical parameters is an important step. The detailed description of the procedure has been reported in the literature (Chakraborty et al 2006; Chakraborty et al., 2014b). In this paper, data was fitted to the kinetic model by non-linear regression analysis using the Marquadt–Levenberg algorithm. The minimum number of parameters required to accurately fit the data was determined by finding the number of components in which the sum of squares of the weighted residuals shown below achieved a minimum value.

$$\text{Sum of squares of the weighted residuals} = \sum \left[ \frac{C(t) - C_T(t)}{C(t)^{1/2}} \right]^2$$

where  $C(t)$  is the experimental value and  $C_T(t)$  is the calculated value using the parameters obtained from the regression analysis. The specific rate constants represent an average value for a group of complexes on a particular site in sediments.

### The lability criteria in Kinetic fractionation study

The concept of *lability* describes the ability of complexes to maintain equilibrium with the free metal ion, M, within the context of an ongoing interfacial process in which a particular species, usually M, is consumed. Consider sediment of  $n$  components, in which each component, designated M-sediment<sub>*i*</sub>, exists in equilibrium with its dissociation products:



Where, where  $k_d$  and  $k_a$  are the rate constants for complex association and dissociation respectively and the thermodynamic stability constant,  $K$ , equals  $k_d/k_a$ .

Under conditions of sufficient excess ligand (L) over metal (M), the association reaction is quasi-monomolecular with rate constant  $k'_d = k_d c_L$ . On time scales,  $t$ , much larger than the characteristic lifetimes of M ( $1/k'_d$ ) and M-sediment<sub>*i*</sub> ( $1/k_a$ ), a given metal ion undergoes frequent interchange between M and M-sediment<sub>*i*</sub>. The complex system is then sufficiently dynamic to maintain bulk equilibrium and obeys the double condition (Gaabass et al., 2009)

$$k'_{dt}, k_{at} \gg 1 \quad (2)$$

In the usual situation of practical interest,  $K' (= K C_{\text{sediment}}) k'_{d}/k_a > 1$ , so Eq. 2 reduces to  $K_{at} \gg 1$ . Thus, metal complexes in sediment will be called labile if their  $k_{at} \gg 1$ .

## Results and discussion

### Variability of dissolved oxygen (DO) concentrations (in bottom water), texture and sedimentary organic carbon content (in sediments) across the OMZ

The various stages of oxygen deficiency in the overlying bottom water (in the study areas) are described in **Table 2**. The sediment samples were purposely collected across the OMZ where the condition of the overlying bottom water changed from oxic to hypoxic and close to suboxic. The distributions of particle size in the underneath sediments are presented in **Table 2**. Coarser particles (sand) (ranging from ~4 to 92%) dominated at the edge of the continental shelf but finer particles (silt+clay) subjugated (ranging from ~8 to 96%) in the sediment collected from the continental slope areas. The sedimentary organic matter (presented as total organic carbon, TOC) content was found to vary from ~1.1 to 8.0 %. A significant positive correlation coefficient was found between the finer sized particles (silt + clay) and TOC ( $r = 0.62$   $p < 0.05$ ,  $n = 10$ ) (Supporting materials, **SM Table 1**) content in the sediments. This indicates that there was high sorption and affinity of TOC on the finer particles in the studied sediments. A similar observation has been reported in the literature (Hedges and Keil, 1995; Paropkari et al., 1987; Chakraborty et al., 2015c). Significant negative correlation was observed between the TOC content in the sediments and the dissolved oxygen (DO) of the overlying bottom water (**Table 4 and supporting materials, SM Figure 1**). It was found that less amount of sedimentary organic matter (represented by TOC) was associated with the finer particles of the sediments under oxic environment. However, preservation of organic matter in the sediment was found to be more under the low oxygen environment. It has been reported that hypoxia of the overlying bottom water may increase organic matter (of higher quality, i.e. less degraded) accumulation and burial in the underneath sediment (Middelburg and Levin, 2009; Nath et al., 1997).

### Distribution of total metals (Cu and Pb) in the surface sediments across the OMZ

The Cu and Pb content in the surface sediments across the OMZ were found to vary from  $19.4 \pm 0.1$  to  $53.1 \pm 0.2$   $\text{mg.kg}^{-1}$  and  $8.0 \pm 0.6$  to  $12.8 \pm 0.1$   $\text{mg.kg}^{-1}$  respectively (**Table 2**). Apparently it seems that varying concentration DO of the overlying bottom water across the OMZ had little effect on the total Cu and Pb content distribution in the studied sediments. However, positive statistical correlation was observed between the TOC content, finer particle (silt+clay) content, and distance from the shore with the total Cu and Pb concentrations in the sediments. It is important to mention that total metal

concentration in the sediment does not provide useful information about their specific chemical forms and their stability in the sediments. Thus, geochemical fractionation and kinetic fractionation studies of Cu and Pb were carried out to understand different geochemical processes that would take place in the sediment under the changing DO concentration of the overlying water across the OMZ in the Arabian Sea.

### **Geochemical fractionation of Cu and Pb in the surface sediments across the OMZ**

Distributions of Cu and Pb in the different binding phases of the studied sediments are shown in **Figure 2a and 2b** and the data (in percentage) are presented in **Table 5**. The lowest fraction of the total concentration of both the metals (vary from 0.1 - 0.9% of the total Cu and ~ 0.0 - 2.7% of the total Pb) in the sediments were present as water soluble complexes.

The fraction of exchangeable and carbonate/bicarbonate forms of Pb and Cu (Fr.2) in the sediments were found to vary from ~0.1 - 2.1% and 0.0 - 21.3% of the total Cu and Pb concentrations in the sediments respectively. Concentrations of Cu and Pb associated with Fe/Mn-oxyhydroxide binding phases (Fr.3) in the sediments were higher than their concentrations in the Fr1 and Fr 2. Scavenging property of Pb by Fe/Mn oxyhydroxide phase in water column and sediment has been identified as an important process in controlling speciation and geochemistry of Pb in marine system (Jones and Turki, 1997; Tessier et al., 1979; Chakraborty et al., 2015a). However, the Fr.2 of Pb was occasionally higher than the Fr.3 in the underneath sediments (off Karwar) where DO concentration of the overlying bottom water was low (Table 5). The fraction of total Pb associated with Fe/Mn oxyhydroxide binding phase gradually increased (~2.8 to 32.9% of the total Pb across the two transects) with the increasing DO level of the overlying bottom water (SM Figure 2). The variations of Pb content (in terms of percentage of the total Pb) in the Fe/Mn oxyhydroxide binding phase against the varying DO level of the overlying bottom water from the two transects are shown separately in the inset (Supporting materials, SM Figure 2).

Compared to Pb, less Cu was bound to Fe/Mn oxyhydroxide (0.7 to 5.0% of the total Cu across the two transects). This indicates that Fe/Mn oxyhydroxide phase in the studied sediments acted as one of the important hosting phases for Pb but not for Cu. Major fractions of the total non residual metal (8.6 – 33.6% of the total Pb and 14.1 to 30.3% of the total Cu) were associated with sedimentary organic matter and sulphides (Fr 4). It was found that Cu had more affinity towards the organic binding phases (including sulphides) than Fe/Mn oxyhydroxide binding phases in the sediments. Strong affinity of Cu for organic binding ligands has already been reported in the literature (Chakraborty et al 2007). Major fractions of the total Pb (~43.7 – 67.3% of the total Pb) and Cu (66.4

– 80.9 % of the total Cu) were present within the structure of the sediments (Fr.5). Sequential extraction study suggested that Cu had strong affinity towards the sedimentary organic phase and major fractions of the non-residual Cu were associated with sedimentary organic matter and sulphides. It was necessary to evaluate the effect of changing bottom-water oxygen concentration (oxic, hypoxic, and close to suboxic) on the geochemical fractionation and the distribution of Cu and Pb in the bottom sediments.

### **Impact of varying dissolved oxygen concentration in the bottom water on geochemical fractionation of Cu and Pb in the sediment**

In this section, the impact of varying dissolved oxygen concentration in the overlying bottom water on geochemical fractionation of Cu and Pb in the underneath sediments are discussed.

**Table 4** indicates that there was a strong positive correlation exists ( $r=0.70$ ,  $p < 0.05$ ,  $n = 10$ ) between the Pb content associated with Fe/Mn-oxyhydroxide binding phase (Pb Fr.3) in the sediment and the dissolved oxygen concentrations of the overlying bottom water. There was a gradual decrease in Pb association (~8.2 to 2.8 % (SSK 71) and 32.9 to 3.8 % (ssk-80) of the total Pb) with Fe/Mn-oxyhydroxide binding phase in the sediment with the decreasing dissolved oxygen concentrations (from ~81.1 to 7.4  $\mu\text{M}$  (SSK-71) and 150.5 to 8.2  $\mu\text{M}$  (SSK-80)) of the overlying bottom water (Table 5 and Supporting materials, SM **Figure 2**).

It is well known that reduction (Fe (III) to Fe (II)) and dissolution of Fe(III) takes place under hypoxic condition (Berner,1981; Lovely and Phillips,1988; Nealson and Saffarini ,1994; Sørensen,1982). Metals (trace/heavy) associated with Fe (III)-oxyhydroxides are expected to be released during dissolution of Fe (III) process under low oxygen environment. Thus, one could expect a gradual decrease of Pb association with Fe (III)-oxyhydroxide phase in the sediments with the decreasing dissolved oxygen level of the overlying bottom water. It is interesting to note that there was a strong negative correlation ( $r=-0.57$ ,  $p < 0.05$ ,  $n = 10$ ) (**Table 4**) existed between the concentration of Pb associated with the sedimentary organic phases (Pb Fr.4) and the dissolved oxygen concentration of the overlying bottom water. Increase in concentration of sedimentary organic matter with decreasing DO level was probably responsible for the increase in Pb association with organic binding phases in the sediment (as shown in the supporting materials, SM **Figure 3**).

The concentration of Cu associated with Fe (III)-oxyhydroxide (Cu Fr.3) in the sediments was positively ( $r=0.97$ ,  $p < 0.05$ ,  $n=10$ ) correlated with the DO concentration of the overlying bottom water (**SM Figure 4**). Association of Cu with Fe (III)-oxyhydroxide in the sediments decreased (~3.0 to 0.8 % (SSK 71) and 5.0 to 0.7 % (ssk-80) of the total Cu) with the decreasing DO concentrations

(from ~81.1 to 7.4  $\mu\text{M}$  (SSK-71) and 150.5 to 8.2  $\mu\text{M}$  (SSK-80)) of the overlying bottom water as shown in supporting materials, SM **Figure 4**. **Table 5** shows that there was increase in Cu association with the sedimentary organic matter (from ~19.2 to 26.8 % (SSK 71) and 14.1 to 30.3 % (SSK-80) of the total Cu) with the decreasing DO level (from ~81.1 to 7.4  $\mu\text{M}$  (SSK-71) and 150.5 to 8.2  $\mu\text{M}$  (SSK-80) of the overlying bottom water (SM **Figure 5**). Slow degradation of organic matter lead to increase preservation of sedimentary organic matter at low oxygen environment in this region. Low DO level in the bottom water might increase the formation of sulphides in the underneath sediment, It was also found that the concentrations of Cu and Pb associated with organic binding phase increased with increasing sulphide concentration in the sediments as shown in supporting materials, SM **Figure 6a and 6b**.

**SM Figure 4** shows a steady decrease in the Cu concentration associated with Fe-Mn oxyhydroxide with decreasing DO concentration of the overlying bottom water in the study area. This is due to the reduction and dissolution of Fe (III)-Mn-oxyhydroxide binding phase in the sediment. Preservation of more organic matter in the sediments under low oxygen environment was also observed. It was found that Cu started accumulating more with the organic binding phases of the sediments with decreasing concentration of dissolved oxygen of the overlying bottom water. However, further geochemical fractionation study of Fe was performed to understand the changes in concentration of Fe-oxyhydroxide binding phase in the studied sediments.

#### **Impact of varying dissolved oxygen concentration in the bottom water on geochemical fractionation of Fe in the surface sediments**

Total concentrations of sedimentary Fe are presented in Table 2. Distributions of different geochemical forms of Fe in the studied sediments (across the OMZ) are presented in **Table 5**. The highest fraction of the total Fe was present in the residual phase (i.e. within the structure of the sediment) in all the sediments. The second highest fraction of the total Fe was associated with organic phase or present as Fe-sulphide. It has been reported that organic matter can trap Fe in marine environment. It was also found that the concentrations of Fe associated with organic binding phase increased with increasing sulphide concentrations in the sediments. Thus, one could expect that sulphide and sedimentary organic matter were the major binding phases for Fe in the sediments. The concentration of Fe(III)-oxyhydroxide (one of the major hosting phases for Pb and Cu ) was found to be the third highest fraction of the total Fe in all the sediment. It is important to note that there was no significant variation of the total sedimentary Fe concentration with varying DO concentrations of the overlying bottom water. However, a significant variation in the concentration of Fe(III)-oxyhydroxide was found with varying DO level of the overlying bottom water.

**Figure 3a and 3b** shows that the concentration of Fe(III)-oxyhydroxides in the surface sediments gradually decreased with the decreasing DO concentration of the overlying bottom water. This is due to increase in reduction of Fe(III) to Fe(II) (and dissolution of Fe(II) from the sediment to the overlying bottom water) with decreasing DO concentration of the bottom water. The similar variation was also found with the concentration of Cu and Pb associated with Fe/Mn-oxyhydroxide binding phases (Fr.3) in the sediments with varying DO concentration of the overlying bottom water. The concentration of Pb and Cu associated with Fe/Mn oxyhydroxide binding phase gradually decreased with the decreasing DO concentration of the overlying bottom water. This is due to increase in reduction of Fe (III) in the sediment with decreasing DO concentration of the overlying bottom water.

Impact of varying dissolved oxygen concentration of the overlying bottom on trace/heavy metals speciation and their release from the underneath sediment in the Arabian Sea is poorly known. Thus, the impact of decreasing DO concentrations of the overlying bottom water on the stability and lability of Cu and Pb complexes in the underneath sediment were further studied.

#### **Impact of varying dissolved oxygen concentration in the overlying bottom water on the stability of Cu and Pb complexes in the underneath sediments**

Kinetic fractionation study was performed to quantitatively estimate the stability and lability of the metal complexes in the underneath sediments across the OMZ. The kinetic extraction data are presented as supporting documents (in **SM Figure 7a and 7b**). The data were fitted to the kinetic model by nonlinear regression analysis, as described elsewhere (Chakraborty et al. 2012; Chakraborty et al. 2011; Gaabass et al. 2009; Hassan et al. 2006; Mandal et al. 2002; Sekaly et al. 1999a; Sekaly et al. 1999b), to obtain the relative percentages of the kinetically distinguishable complexes and their associated dissociation rate constants. The percentage of labile and inert complexes of Cu and Pb and their corresponding dissociation rate coefficients are presented as supporting document (SM Table 2). **Figure 4a and 4b** show the variation in percentages of labile metal complexes and their dissociation rate constants (**Figure 4 c and 4d**) in the sediments against the changing DO concentration of the overlying bottom water.

The kinetic fractionation study indicates that Cu-sediment complexes were stronger than the Pb-sediment complexes under low oxygen environment. The decrease in bottom water DO (from 81.1 to 7.4  $\mu\text{M}$ ) decreased the fractions of labile Cu-complexes from 6.3 to 3.7 % of the total Cu in the underneath sediments. The corresponding dissociation rate constant of the Cu-sediment complexes was found to change from  $1.8 \times 10^{-3}$  to  $3.9 \times 10^{-3} \text{ s}^{-1}$ . This study indicates that the lability and

dissociation rate constants of Cu-sediment complexes gradually decreased (i.e. stability of the Cu-sediment complexes steadily increased) with the decreasing DO concentration of the overlying bottom water.

It was found that the lability and dissociation rate constant of Pb-sediment complexes increased with the decreasing DO concentration in the overlying bottom water. The change in DO concentration from 7.6 to 81.1  $\mu\text{M}$  increased the concentration of labile Pb-complexes from 19.8 to 27.0 % of the total Pb content in the sediment. The dissociation rate constant of the Pb-sediment complexes was found to increase from  $5.9 \times 10^{-3}$  to  $7.9 \times 10^{-3} \text{ s}^{-1}$ . Although the results from the kinetic fractionation experiments are operationally defined, the observed trends in metal lability in sediment as a function DO concentration of the overlying water column elucidate the relative stability of metal-sediment complexes across the OMZ. This study suggests that low oxygen environment in the overlying bottom water may increase lability of Pb-sediment complexes in the underneath sediment and may increase bioavailability of Pb in the system.

### **Conclusions:**

This study provided useful information on the impact of varying dissolved oxygen concentration in overlying bottom water on geochemical fractionation of Cu and Pb complexes in the underneath sediments across the OMZ, in the eastern Arabian Sea. Increasing concentration of sedimentary organic matter (under low oxygen environment of the overlying bottom water) increased Cu complexation and association of Cu with the organic binding phases of the sediment. The average stability of Cu-sediment complexes was found to increase with decreasing dissolved oxygen concentrations of overlying bottom water. However, association of Pb with Fe-Mn-oxyhydroxide phase gradually decreased with decreasing dissolved oxygen concentration of the overlying bottom water. Pb was found to associate with sedimentary organic matter under the low oxygen environment. The lability of Pb-sediment complexes gradually increased with decreasing dissolved oxygen concentrations of bottom water. The labile Pb-sediment complexes may participate in exchange fluxes at the continent-ocean interface at the low oxygen environment in the western continental margin of India.

### ***Acknowledgments***

Authors are thankful to the Director, NIO, Goa, for his encouragement and support. Dr Priyanka Banerjee is gratefully acknowledged for her discussion about the study areas. All the shipboard scientific staff of R.V.Sindhu Sankalp cruises 71 and 80 are sincerely acknowledged for their help in collecting the water and sediment samples. Drs. C.Prakash Babu and V.Ramaswamy are thanked for

Coulometer and Elemental Analyser facilities. This work is a part of the Council of Scientific and Industrial Research (CSIR) supported GEOSINKS (PSC0106) project. This article bears NIO contribution number XXXX.

## References

Alvarez, E. A., Mochon, M. C., Sánchez, J. J., & Rodríguez, M. T. (2002). Heavy metal extractable forms in sludge from wastewater treatment plants. *Chemosphere*, 47(7), 765-775.

Banse, K., Naqvi, S. W. A., Narvekar, P. V., Postel, J. R., & Jayakumar, D. A. (2014). Oxygen minimum zone of the open Arabian Sea: variability of oxygen and nitrite from daily to decadal timescales. *Biogeosciences*, 11, 2237–2261.

Belzile, N., Lecomte, P. and Tessier, A., 1989. Testing readsorption of trace elements during partial chemical extractions of bottom sediments. *Environmental science & technology*, 23(8),1015-1020.

Berner, R.A., 1981. A new geochemical classification of sedimentary environments. *Journal of Sedimentary Research*, 51(2) 359-365.

Broenkow, W.W. and Cline, J.D., 1969. Colorimetric determination of dissolved oxygen at low concentrations. *Limnology and Oceanography*, 14(3), pp.450-454.

Bryan, J.R., Riley, J.P. and Williams, P.L., 1976. A Winkler procedure for making precise measurements of oxygen concentration for productivity and related studies. *Journal of Experimental Marine Biology and Ecology*, 21(3), pp.191-197.

Calmano, W., Hong, J. and Förstner, U., 1993. Binding and mobilization of heavy metals in contaminated sediments affected by pH and redox potential. *Water science and technology*, 28,223-223.

Chakraborty, P., Gopalapillai, Y., Murimboh, J., Fasfous, I.I. and Chakrabarti, C.L., 2006. Kinetic speciation of nickel in mining and municipal effluents. *Analytical and Bioanalytical chemistry*, 386(6),1803-1813.

Chakraborty, P., Fasfous, I.I., Murimboh, J. and Chakrabarti, C.L., 2007. Simultaneous determination of speciation parameters of Cu, Pb, Cd and Zn in model solutions of Suwannee River fulvic acid by pseudopolarography. *Analytical and Bioanalytical Chemistry*, 388(2), 463-474.

Chakraborty, P., Babu, P.R. and Sarma, V.V., 2011. A multi-method approach for the study of lanthanum speciation in coastal and estuarine sediments. *Journal of Geochemical Exploration*, 110(2), 225-231.

Chakraborty, P., 2012. Speciation of Co, Ni and Cu in the coastal and estuarine sediments: Some fundamental characteristics. *Journal of Geochemical Exploration*, 115, 13-23.

Chakraborty, P., Babu, P.R. and Sarma, V.V., 2012. A study of lead and cadmium speciation in some estuarine and coastal sediments. *Chemical Geology*, 294, 217-225.

Chakraborty, P., Chakraborty, S., Ramteke, D. and Chennuri, K., 2014. Kinetic speciation and bioavailability of copper and nickel in mangrove sediments. *Marine Pollution Bulletin*, 88(1), 224-230.

Chakraborty, P., Babu, P.R., Vudamala, K., Ramteke, D. and Chennuri, K., 2014a. Mercury speciation in coastal sediments from the central east coast of India by modified BCR method. *Marine Pollution Bulletin*, 81(1), pp.282-288.

Chakraborty, P., Manek, A., Niyogi, S. and Hudson, J., 2014b. Determination of dynamic metal complexes and their diffusion coefficients in the presence of different humic substances by combining two analytical techniques. *Analytical Letters*, 47(7), 1224-1241.

Chakraborty, P., Ramteke, D. and Chakraborty, S., 2015a. Geochemical partitioning of Cu and Ni in mangrove sediments: Relationships with their bioavailability. *Marine Pollution Bulletin*, 93, 194-201.

Chakraborty, S., Chakraborty, P. and Nath, B.N., 2015 b. Lead distribution in coastal and estuarine sediments around India. *Marine Pollution Bulletin*, 97(1), pp.36-46.

Chakraborty, P., Sarkar, A., Vudamala, K., Naik, R. and Nath, B.N., 2015 c. Organic matter—a key factor in controlling mercury distribution in estuarine sediment. *Marine Chemistry*, 173, pp.302-309.

Chakraborty, P., Chakraborty, S., Vudamala, K., Sarkar, A. and Nath, B.N., 2016. Partitioning of metals in different binding phases of tropical estuarine sediments: importance of metal chemistry. *Environmental Science and Pollution Research*, 23, 4, 3450-3462

de Boyer Montégut, C., Madec, G., Fischer, A. S., Lazar, A., & Iudicone, D., 2004. Mixed layer depth over the global ocean: An examination of profile data and a profile-based climatology. *Journal of Geophysical Research: Oceans*, 109(C12).

Flemming, C.A. and Trevors, J.T., 1989. Copper toxicity and chemistry in the environment: a review. *Water, Air, & Soil Pollution*, 44(1), pp.143-158.

Gaabass, I., Murimboh, J.D. and Hassan, N.M., 2009. A study of diffusive gradients in thin films for the chemical speciation of Zn (II), Cd (II), Pb (II), and Cu (II): The role of kinetics. *Water, air, and soil pollution*, 202(1-4), 131-140.

Graetz, D. A., Keeney, D. R., & Aspiras, R. B., 1973. Eh status of lake sediment-water systems in relation to nitrogen transformations I. *Limnology and Oceanography*, 18(6), 908-917.

Hanson Jr, A. K., & Quinn, J. G. (1983). The distribution of dissolved and organically complexed copper and nickel in the Middle Atlantic Bight. *Canadian Journal of Fisheries and Aquatic Sciences*, 40(S2), s151-s161.

Hassan, N.M., Murimboh, J.D., Sekaly, A.L., Mandal, R., Chakrabarti, C.L. and Grégoire, D.C., 2006. Cascade ultrafiltration and competing ligand exchange for kinetic speciation of aluminium, iron, and nickel in fresh water. *Analytical and Bioanalytical chemistry*, 384(7-8), 1558-1566.

Hedges, J.I. and Keil, R.G., 1995. Sedimentary organic matter preservation: an assessment and speculative synthesis. *Marine Chemistry*, 49(2), 81-115.

Henrichs, S.M. and Reeburgh, W.S., 1987. Anaerobic mineralization of marine sediment organic matter: rates and the role of anaerobic processes in the oceanic carbon economy. *Geomicrobiology Journal*, 5(3-4), 191-237.

<http://www.cdc.gov/niosh/docs/2003-154/pdfs/7105.pdf>

Jahnke, R.A., Emerson, S.R. and Murray, J.W., 1982. A model of oxygen reduction, denitrification, and organic matter mineralization in marine sediments I. *Limnology and Oceanography*, 27(4), 610-623.

Jones, B., & Turki, A. (1997). Distribution and speciation of heavy metals in surficial sediments from the Tees Estuary, north-east England. *Marine Pollution Bulletin*, 34(10), 768-779.

Kamykowski, D., & Zentara, S. J., 1990. Hypoxia in the world ocean as recorded in the historical data set. *Deep Sea Research Part A. Oceanographic Research Papers*, 37(12), 1861-1874.

Prasanna Kumar, S., Narvekar, J., Kumar, A., Shaji, C., Anand, P., Sabu, P., & Nair, K. K. C., 2004. Intrusion of the Bay of Bengal water into the Arabian Sea during winter monsoon and associated chemical and biological response. *Geophysical Research Letters*, 31(15).

Kwon, Y.T. and Lee, C.W., 2001. Ecological risk assessment of sediment in wastewater discharging area by means of metal speciation. *Microchemical Journal*, 70(3), 255-264.

Lovley, D.R., 1987. Organic matter mineralization with the reduction of ferric iron: a review. *Geomicrobiology Journal*, 5(3-4), pp.375-399.

Lovley, D.R. and Phillips, E.J., 1988. Novel mode of microbial energy metabolism: organic carbon oxidation coupled to dissimilatory reduction of iron or manganese. *Applied and environmental microbiology*, 54(6), 1472-1480.

Luoma, S. N., & Bryan, G. W. (1981). A statistical assessment of the form of trace metals in oxidized estuarine sediments employing chemical extractants. *Science of the Total Environment*, 17(2), 165-196.

Mandal, R., Hassan, N. M., Murimboh, J., Chakrabarti, C. L., Back, M. H., Rahayu, U., & Lean, D. R. (2002). Chemical speciation and toxicity of nickel species in natural waters from the Sudbury area (Canada). *Environmental science & technology*, 36(7), 1477-1484.

Middelburg, J. J., & Levin, L. A. (2009). Coastal hypoxia and sediment biogeochemistry. *Biogeosciences*, 6.1273–1293

Morrison, J.M., Codispoti, L.A., Smith, S.L., Wishner, K., Flagg, C., Gardner, W.D., Gaurin, S., Naqvi, S.W.A., Manghnani, V., Prosperie, L. and Gundersen, J.S., 1999. The oxygen minimum zone in the Arabian Sea during 1995. *Deep Sea Research Part II: Topical Studies in Oceanography*, 46(8), pp.1903-1931.

Muraleedharan, P. M., & Prasannakumar, S., 1996. Arabian Sea upwelling-A comparison between coastal and open ocean regions, *Current Science*, 70 (11), 842-846.

Naqvi, S.W.A. and Noronha, R.J., 1991. Nitrous oxide in the Arabian Sea. *Deep Sea Research Part A. Oceanographic Research Papers*, 38(7), 871-890.

Nath, B.N., Bau, M., Rao, B.R. and Rao, C.M., 1997. Trace and rare earth elemental variation in Arabian Sea sediments through a transect across the oxygen minimum zone. *Geochimica et Cosmochimica Acta*, 61(12), pp.2375-2388.

Nealson, K.H. and Saffarini, D., 1994. Iron and manganese in anaerobic respiration: environmental significance, physiology, and regulation. *Annual Reviews in Microbiology*, 48(1), pp.311-343.

Olson, D.L. and Shuman, M.S., 1985. Copper dissociation from estuarine humic materials. *Geochimica et Cosmochimica Acta*, 49(6), 1371-1375.

Paropkari, A.L., Rao, C.M. and Murty, P.S.N., 1987. Environmental controls on the distribution of organic matter in recent sediments of the western continental margin of India. *Petroleum geochemistry and exploration in Afro-Asian Region*, 347-361.

Pedersen, T.F. and Calvert, S.E., 1990. Anoxia vs. productivity: what controls the formation of organic-carbon-rich sediments and sedimentary Rocks?(1). *AAPG Bulletin*, 74(4), 454-466.

Ramaswamy, V., & Rao, P. S., 2006. Grain size analysis of sediments from the northern Andaman Sea: comparison of laser diffraction and sieve-pipette techniques. *Journal of Coastal Research*, 1000–1009

Sekaly, A.L., Mandal, R., Hassan, N.M., Murimboh, J., Chakrabarti, C.L., Back, M.H., Gregoire, D.C. and Schroeder, W.H., 1999a. Effect of metal/fulvic acid mole ratios on the binding of Ni (II), Pb (II), Cu (II), Cd (II), and Al (III) by two well-characterized fulvic acids in aqueous model solutions. *Analytica Chimica Acta*, 402(1), 211-221.

Sekaly, A.L., Chakrabarti, C.L., Back, M.H., Gregoire, D.C., Lu, J.Y. and Schroeder, W.H., 1999b. Stability of dissolved metals in environmental aqueous samples: Rideau River surface water, rain and snow. *Analytica chimica acta*, 402(1), 223-231.

Shetye, S. R., Gouveia, A. D., & Shenoi, S. S. C., 1994. Circulation and water masses of the Arabian Sea. *Proceedings of the Indian Academy of Sciences-Earth and Planetary Sciences*, 103(2), 107-123.

Sørensen, J., 1982. Reduction of ferric iron in anaerobic, marine sediment and interaction with reduction of nitrate and sulfate. *Applied and Environmental Microbiology*, 43(2), pp.319-324.

Tack, F.M.G. and Verloo, M.G., 1995. Chemical speciation and fractionation in soil and sediment heavy metal analysis: a review. *International Journal of Environmental Analytical Chemistry*, 59(2-4), pp.225-238.

Tessier, A., Campbell, P. G., & Bisson, M., 1979. Sequential extraction procedure for the speciation of particulate trace metals. *Analytical Chemistry*, 51(7), 844-851.

Welcher F.J., *The Analytical uses of Ethylenediaminetetraacetic Acid*, D. Van Nostrand Company, Inc., Toronto, Canada, 1958, Chapter 1.

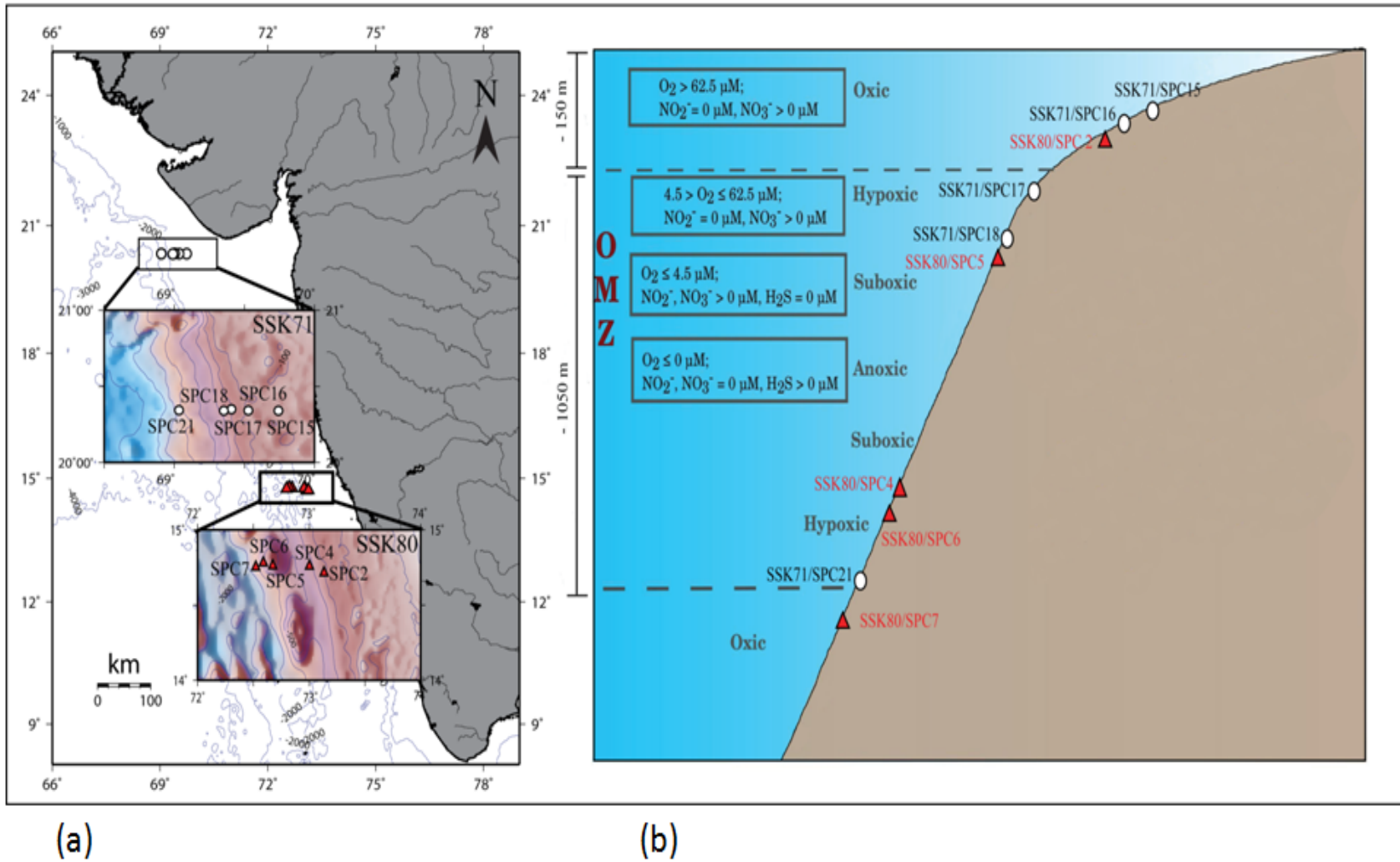


**Figure 1: Study area:** Sediment samples were collected from (a) the continental margin off Karwar (SSK#80) and off Gujarat (SSK#71), west coast of India; (b) Schematic diagram of sampling locations with respect to depth and oxygen concentrations.

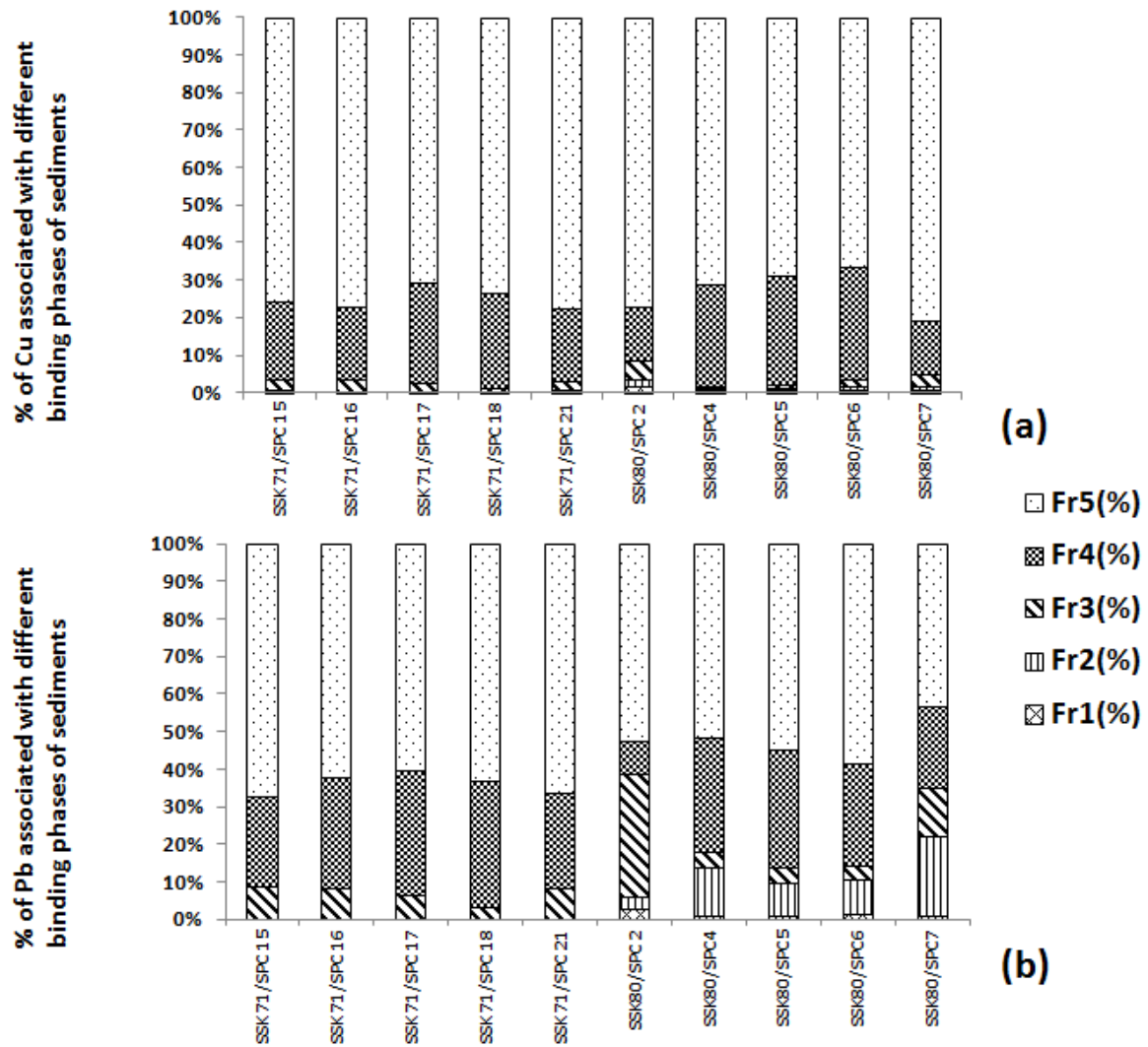


**Figure 2:** Distributions of Cu (a) and Pb (b) in different binding phases of the studied sediments across the OMZ

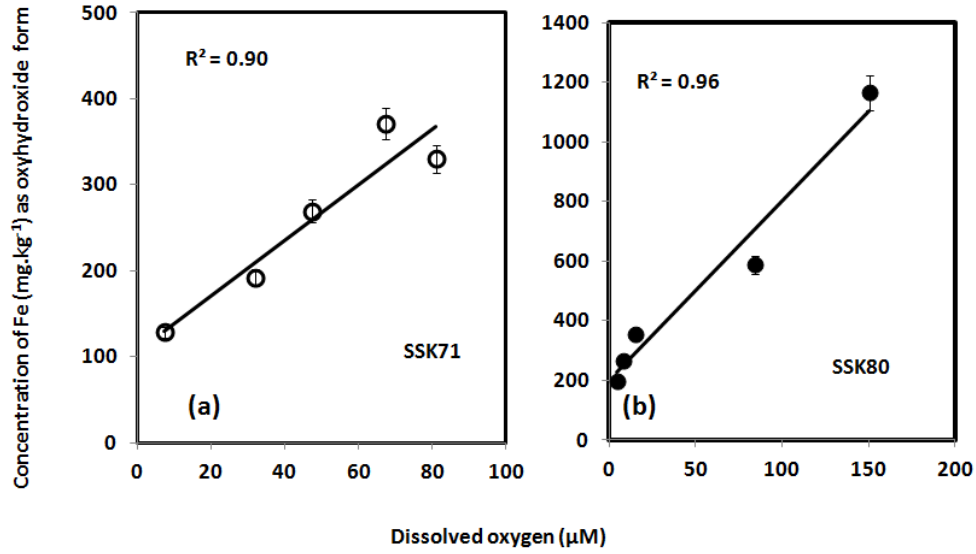


**Figure 3:** variation of the concentration of oxyhydroxide form of Fe ( $\text{mg.kg}^{-1}$ ) in the studied sediment with varying bottom water oxygen concentration (DO) ( $\mu\text{M}$ )

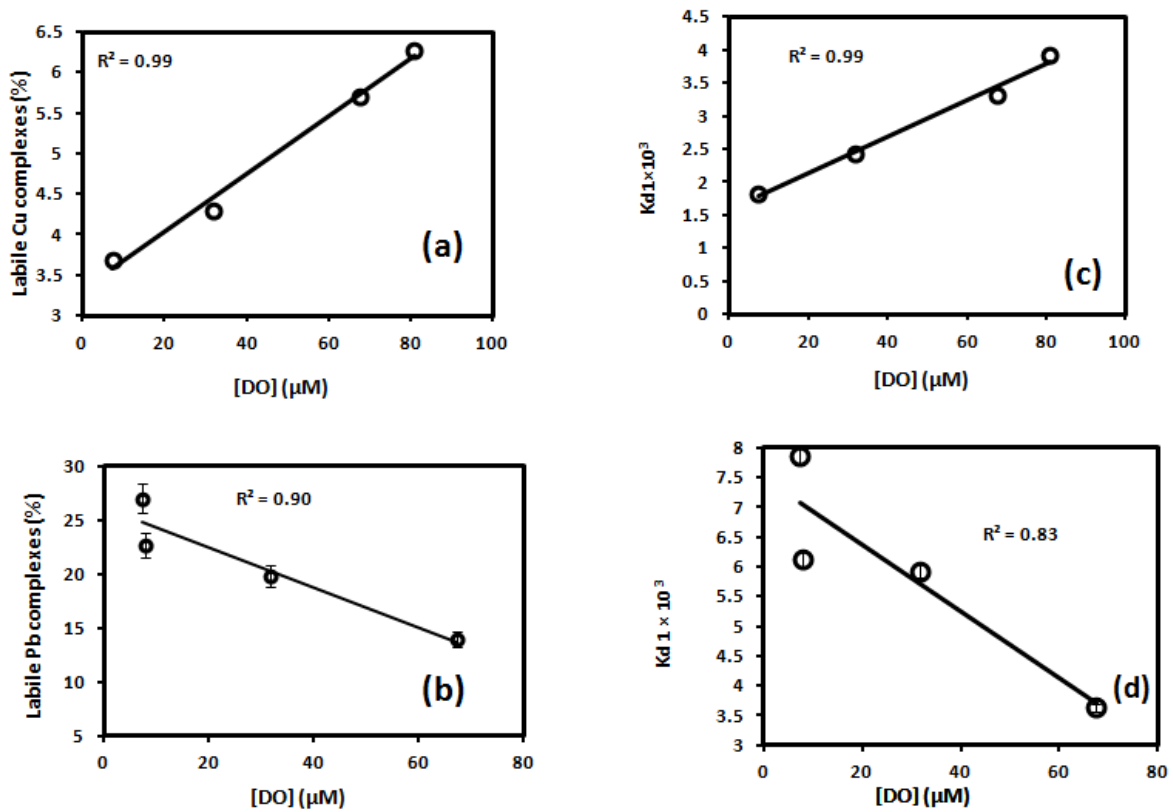


**Figure 4:** variation in concentrations of labile complexes and their dissociation rate constants of (a and c) Cu and (b and d) Pb against the dissolved oxygen (DO) ( $\mu\text{M}$ ) concentration of the overlying bottom water

Table 1: The description of oxic, hypoxic, suboxic conditions are defined below (Naqvi et al 2010).

Stage	Criteria
Oxic	$O_2 > 62.49 \mu M^*$ ; $NO_2^- = 0 \mu M$ , $NO_3^- > 0 \mu M$
Hypoxia	$4.46 < O_2 \leq 62.49 \mu M$ ; $NO_2^- = 0 \mu M$ , $NO_3^- > 0 \mu M$
Suboxia	$O_2 = 4.46 \mu M$ , $NO_2^-$ , $NO_3^- > 0 \mu M$ ; $H_2S = 0 \mu M$
Anoxia	$O_2 = 0 \mu M$ , $NO_2^-$ , $NO_3^- = 0 \mu M$ ; $H_2S > 0 \mu M$

\*  $1 \text{ ml l}^{-1} = 1.43 \text{ mg l}^{-1} = 44.66 \mu M$

TEXTURE (sand,silt+clay)(%), total Pb, Cu and Fe (mg.kg

Table 2

Geographical locations of sediment sampling sites, depth, temperature, salinity, dissolved oxygen (DO), redox state of the overlying bottom water, and concentration of TOC, texture (sand, silt + clay), total Pb, Cu and Fe in the studied sediment.

Station	LAT (°N)	LONG (°E)	Depth (m)	Temp. (°C)	Salinity (PSU)	DO ( $\mu$ M)	Redox state	TOC (%)	Particle size		Pb (mg.kg <sup>-1</sup> )	Cu (mg.kg <sup>-1</sup> )	Fe (mg.kg <sup>-1</sup> )
									Sand (%)	Silt+Clay (%)			
SSK71/SPC15	20 20.44	69 44.54	80	23.6	36.4	81.1	Oxic	1.1	77	23	9.6±0.4	35.0±1.3	74158
SSK71/SPC16	20 20.56	69 31.71	98	22.9	36.4	67.5	Oxic	1.1	92	8	8.0±0.6	27.2±0.8	65856
SSK71/SPC17	20 20.98	69 24.48	195	19.9	35.9	32.0	Hypoxic	2.5	58	42	11.3±0.9	36.2±1.3	54891
SSK71/SPC18	20 20.40	69 21.19	297	14.8	35.8	7.4	Hypoxic	3.8	45	55	8.8±0.1	39.7±0.4	73446
SSK71/SPC 21	20 20.64	69 02.052	1544	5.3	35.1	47.3	Hypoxic	3.4	4	96	9.8±1.4	50.3±1.4	63151
SSK80/SPC 2	14 43.72	73 18.93	110	26.8	39.2	150.5	Oxic	1.0	59	41	12.8±0.1	19.4±0.1	33210
SSK80/SPC4	14 45.52	73 00.19	563	10.9	37.2	8.2	Hypoxic	6.5	5	95	12.1±1.3	41.7±0.1	30940
SSK80/SPC5	14 45.65	72 40.45	329	12.7	37.1	4.7	Close to suboxic	8.0	14	86	11.5±0.4	35.4±1.8	31050
SSK80/SPC6	14 46.79	72 35.42	682	11.3	38.1	14.9	Hypoxic	6.8	24	76	11.9±0.3	31.7±1.8	22260
SSK80/SPC7	14 45.15	72 31.24	1711	4.1	37.9	84.6	Oxic	1.7	6	94	10.0±1.1	39.6±0.2	36760

The concentrations of Pb and Cu are expressed as mean ± standard deviation (n=3)

Table 3

Optimized instrumental conditions for the determination of Cu, Pb (by ETAAS) and Fe (by flame AAS) in the studied sediment. Optimized conditions of flame AAS for the determination of sedimentary Fe is also given below

	Step	Description	Temp (°C)	Ramp time (s)	Hold time (s)	Internal flow	Gas-flow type
Cu	1	Initial drying	110	1	30	250	Normal
	2	Final drying	130	15	30	250	Normal
	3	Ashing	1200	10	20	250	Normal
	4	Atomization	2000	0	5	0	No flow
	5	cleanout	2450	1	3	250	Normal
Pb	1	Initial Drying	110	1	30	250	Normal
	2	Final Drying	130	15	30	250	Normal
	3	Ashing	850	10	20	250	Normal
	4	Atomization	1600	0	5	0	No flow
	5	cleanout	2450	1	3	250	Normal

Table 4

The Pearson correlation between the dissolved oxygen (DO) of the overlying bottom water against the total organic carbon (TOC), Cu associated with Fe/Mn-oxyhydroxide (Cu Fr.3), Cu associated with organic binding phase (Cu Fr. 4), Pb associated with Fe/Mn oxyhydroxide (Pb Fr. 3), Pb associated with organic binding phase (Pb Fr. 4), Fe in the form of Fe/Mn-oxyhydroxide (Fe Fr.3) and Fe associated with organic binding phases (Fe Fr.4) in the underneath sediment AAS for the determination of sedimentary Fe is also given below

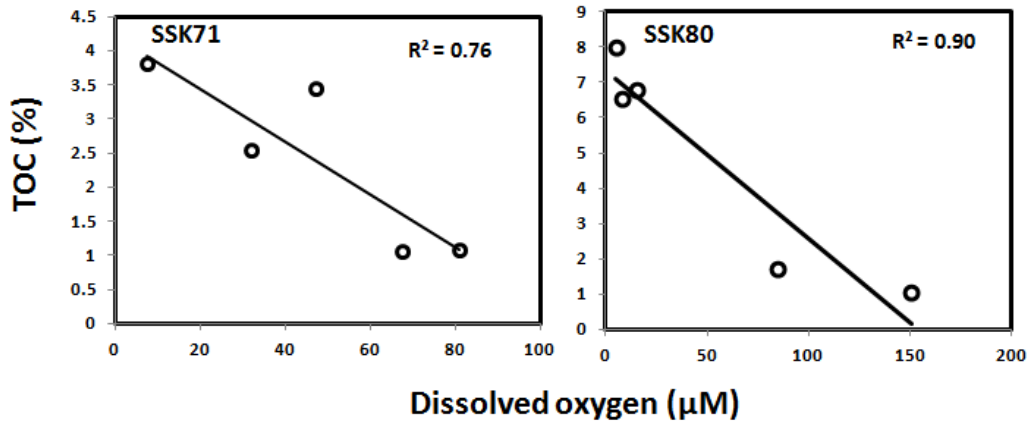
	DO( $\mu$ M)	TOC(%)	Cu.Fr3	Cu.Fr4	Pb.Fr3	Pb.Fr4	Fe.Fr3	Fe.Fr4
DO( $\mu$ M)	1.00							
TOC(%)	-0.78	1.00						
Cu.Fr3	0.40	-0.38	1.00					
Cu.Fr4	-0.82	0.82	-0.21	1.00				
Pb.Fr3	0.64	-0.12	0.20	-0.28	1.00			
Pb.Fr4	-0.48	0.40	-0.46	0.55	-0.38	1.00		
Fe.Fr3	0.89	-0.46	0.36	-0.58	0.91	-0.46	1.00	
Fe.Fr4	-0.02	0.48	-0.37	0.39	0.60	0.09	0.34	1.00

Table 5

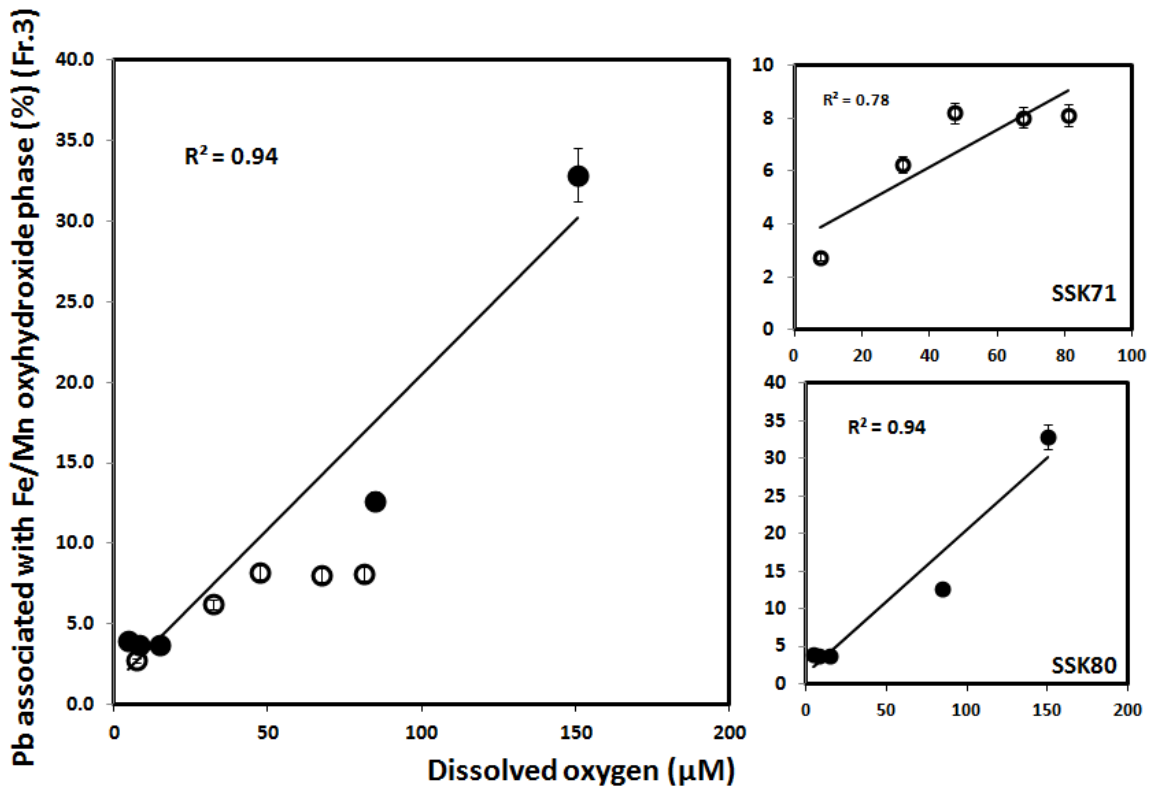
Percentage of total Cu and Pb and the concentration of Fe in different binding phases of the studied sediments across the OMZ.

	Station	DO ( $\mu\text{M}$ )	Fr1(%)	Fr2(%)	Fr3(%)	Fr4(%)	Fr5(%)
Cu	SSK71/SP C15	81.1	0.0	0.5	2.9	20.9	75.6
	SSK71/SP C16	67.5	0.0	0.3	3.0	19.5	77.1
	SSK71/SP C17	32.0	0.1	0.1	2.2	26.8	70.8
	SSK71/SP C18	7.4	0.1	0.1	0.8	25.3	73.7
	SSK71/SP C 21	47.3	0.5	0.1	2.6	19.2	77.7
	SSK80/SPC 2	150.5	1.5	2.1	5.0	14.1	77.4
	SSK80/SPC4	8.2	0.5	0.6	0.7	26.8	71.4
	SSK80/SPC5	4.7	0.6	0.7	0.8	29.1	68.8
	SSK80/SPC6	14.9	0.8	0.9	1.7	30.3	66.4
	SSK80/SPC7	84.6	0.9	0.7	3.4	14.1	80.9
	SSK71/SP C15	81.1	0.2	0.1	8.1	24.3	67.3
	SSK71/SP C16	67.5	0.0	0.3	8.0	29.1	62.6
	SSK71/SP C17	32.0	0.0	0.2	6.2	32.9	60.7
	SSK71/SP C18	7.4	0.0	0.1	2.8	33.6	63.5
Pb	SSK71/SP C 21	47.3	0.0	0.0	8.2	25.1	66.7
	SSK80/SPC 2	150.5	2.7	2.9	32.9	8.6	52.9
	SSK80/SPC4	8.2	0.7	13.1	3.8	30.4	52.0
	SSK80/SPC5	4.7	0.8	8.8	4.0	31.5	54.9
	SSK80/SPC6	14.9	1.0	9.4	3.8	27.0	58.8
	SSK80/SPC7	84.6	0.7	21.3	12.6	21.7	43.7
	Station	DO ( $\mu\text{M}$ )	Fr1( $\text{mg.kg}^{-1}$ )	Fr2( $\text{mg.kg}^{-1}$ )	Fr3( $\text{mg.kg}^{-1}$ )	Fr4( $\text{mg.kg}^{-1}$ )	Fr5( $\text{mg.kg}^{-1}$ )
Fe	SSK71/SP C15	81.1	2.1	37.4	329.9	278.2	73510
	SSK71/SP C16	67.5	3.7	10.9	370.9	180.8	65290
	SSK71/SP C17	32.0	13.4	13.7	192.2	541.1	54130
	SSK71/SP C18	7.4	3.9	16.3	128.4	1237.8	72060
	SSK71/SP C 21	47.3	11.9	16.3	269.2	1083.8	61770
	SSK80/SPC 2	150.5	0.0	41.6	1166.6	1927.3	30074
	SSK80/SPC4	8.2	0.0	12.3	267.8	1267.6	29392
	SSK80/SPC5	4.7	0.0	20.3	197.0	1552.2	29280
	SSK80/SPC6	14.9	0.0	23.3	356.4	1080.4	20799
	SSK80/SPC7	84.6	0.0	14.6	588.0	397.5	35759

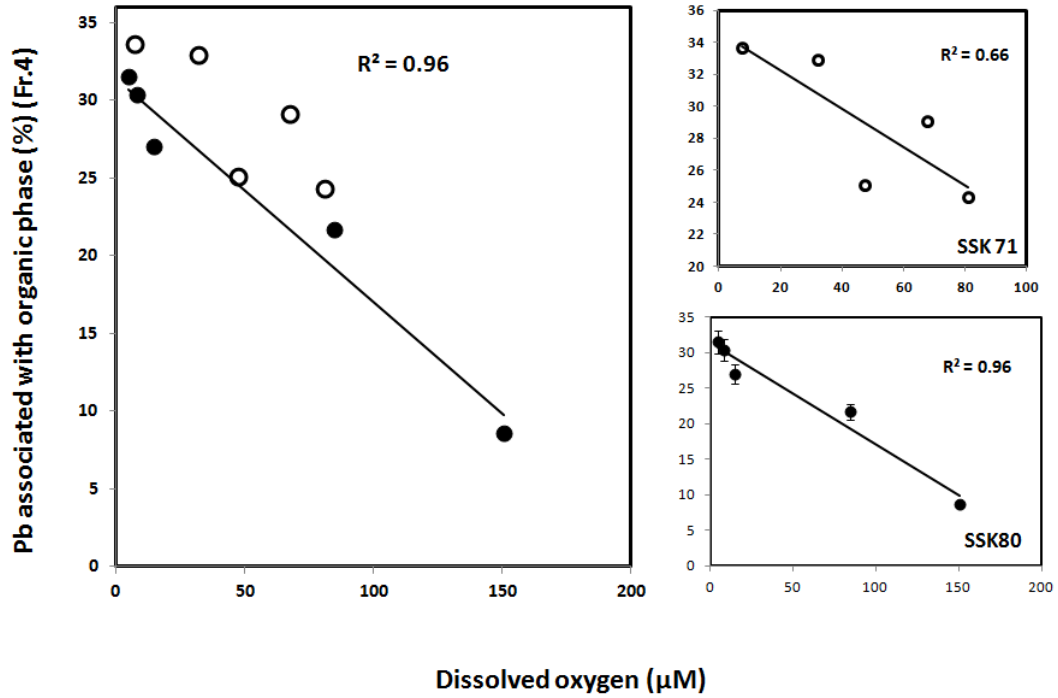
## SUPPORTING DOCUMENTS



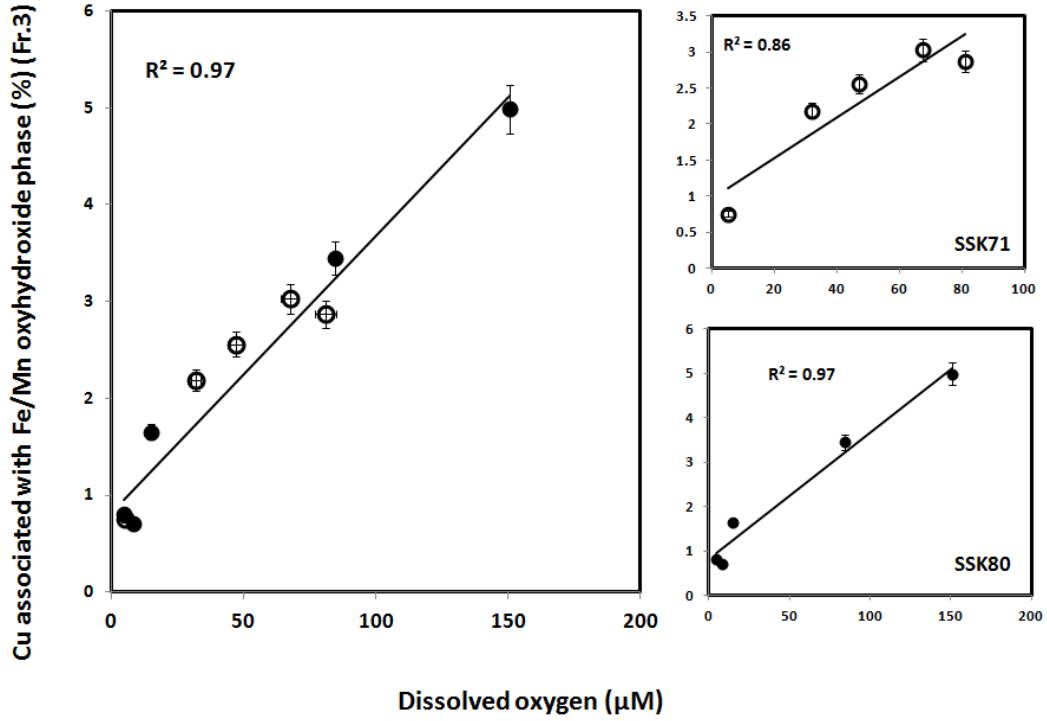
SM Figure 1: Variation of total organic carbon (TOC) (%) with varying bottom water oxygen concentration (DO) (μM)



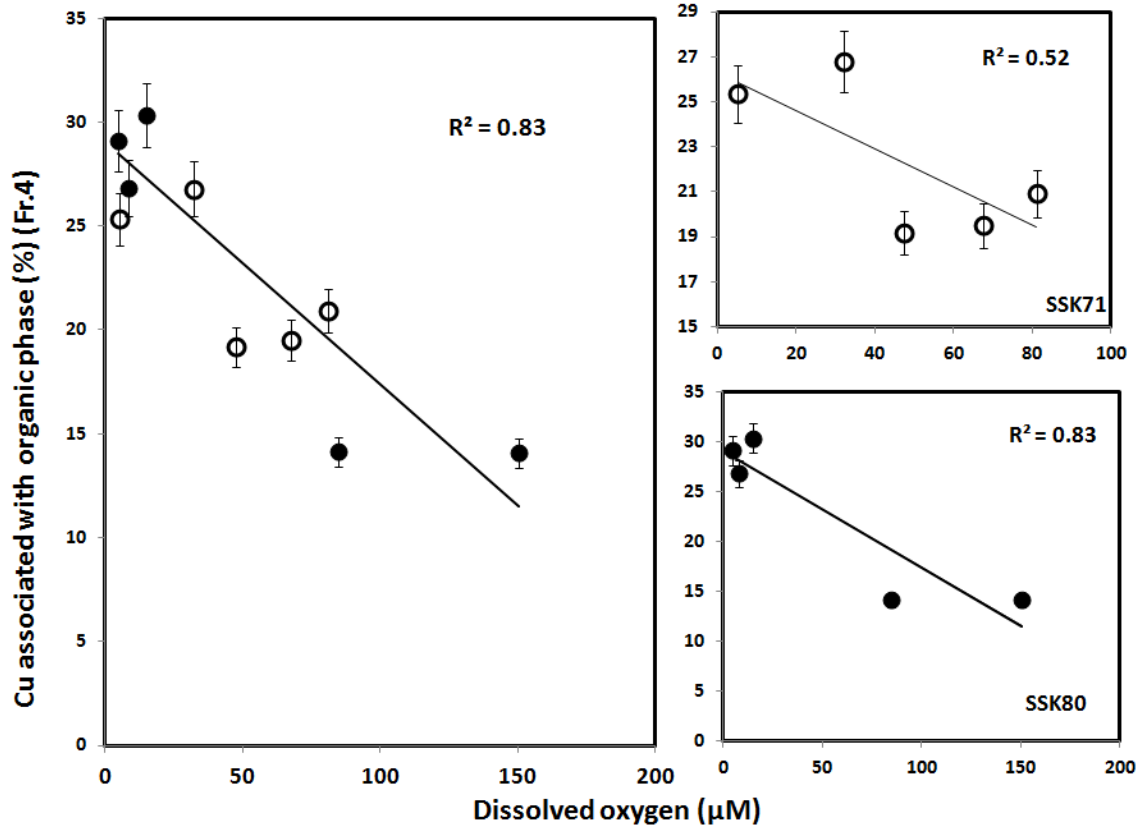
SM Figure 2: variation of Pb (%) in Fe-Mn oxy-hydroxide phase in the studied sediment with varying bottom water oxygen concentration (DO)(μM)



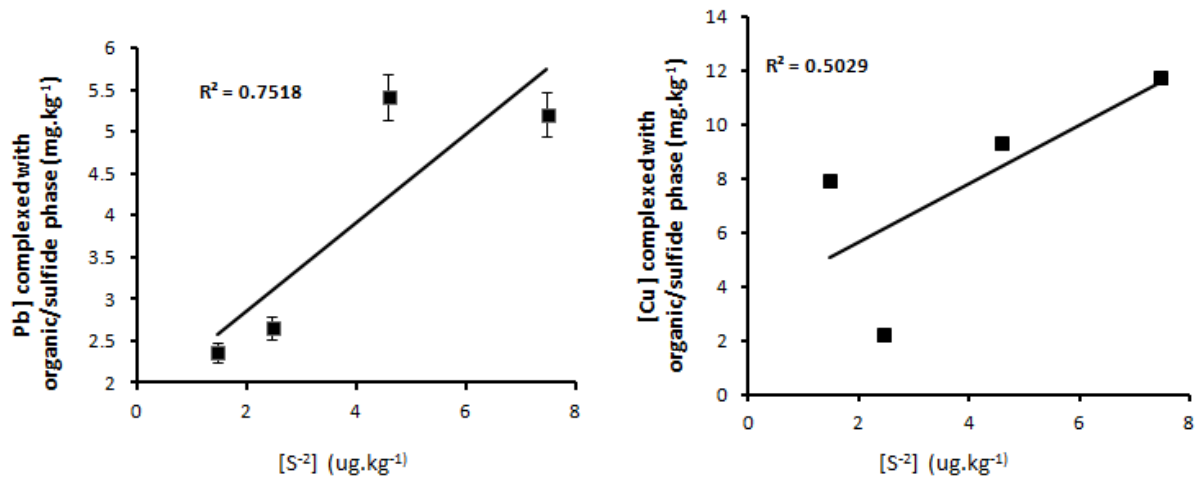
**SM Figure 3 :** variation of Pb (%) in organic phase in the studied sediment with varying bottom water oxygen concentration (DO)( µM)



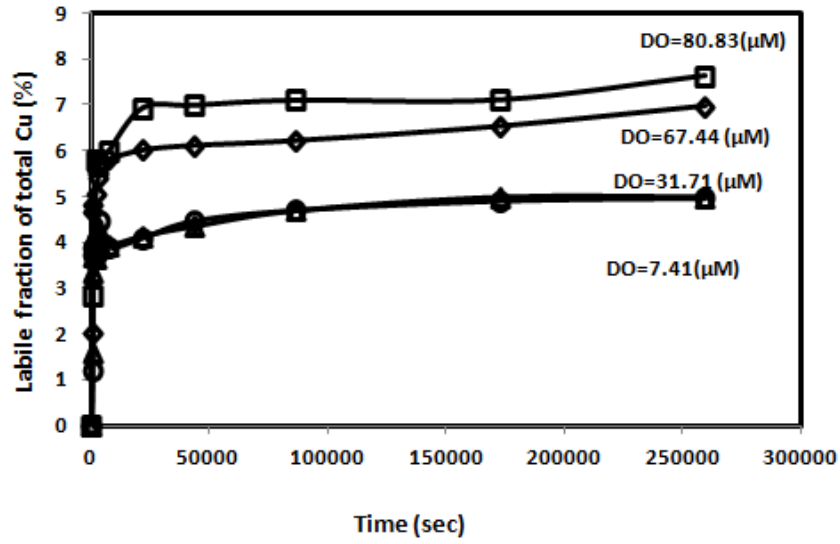
**SM Figure 4:** variation of Cu (%) in Fe/Mn oxyhydroxide phase in the studied sediment with varying bottom water oxygen concentration (DO)( µM)



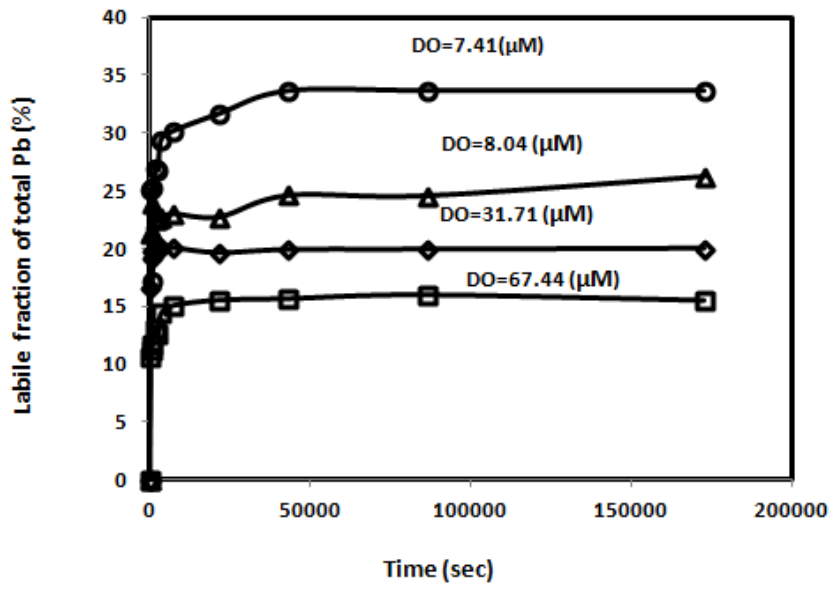
**SM Figure 5:** variation of Cu (%) in organic phase in the studied sediment with varying bottom water oxygen concentration (DO) ( $\mu\text{M}$ )



**SM Figure 6:** variation of (a) Pb ( $\text{mg.kg}^{-1}$ ) and (b) Cu ( $\text{mg.kg}^{-1}$ ) in the sedimentary organic phase as a function of sulfide concentration ( $\mu\text{g.kg}^{-1}$ )



(a)



(b)

SM Figure 7: The percentage of total (a) Cu and (b) Pb released from the studies sediment with time (sec)

**SM Table 1:** Pearson correlation coefficient between the finer particles (silt + clay) and TOC  
Correlation is significant at the 0.05 level (2 tailed)

	<i>sand%</i>	<i>Silt%</i>	<i>clay%</i>	<i>Silt+clay</i>	<i>TOC</i>
sand%	1				
Silt%	-0.93	1			
clay%	-0.95	0.77	1		
Silt+clay	-1	0.93	0.95	1	
TOC	-0.62	<b>0.68</b>	<b>0.50</b>	<b>0.62</b>	1

**SM Table 2.** The percentage of labile (C<sub>1</sub>) and inert (C<sub>2</sub>) complexes of Cu and Pb and their corresponding dissociation rate coefficients (K<sub>d1</sub> and K<sub>d2</sub> respectively)

	<b>Station</b>	<b>C<sub>1</sub> (labile)(%)</b>	<b>K<sub>d1</sub> (S<sup>-1</sup>)</b>	<b>C<sub>2</sub>( inert)(%)</b>	<b>K<sub>d2</sub>×10<sup>7</sup>(S<sup>-1</sup>)</b>
<b>Cu</b>	<b>SSK71/SPC15</b>	<b>5.7</b>	<b>3.3 ×10<sup>-3</sup></b>	<b>94.3</b>	<b>&lt;10<sup>-6</sup></b>
	<b>SSK71/SPC16</b>	<b>6.3</b>	<b>3.9 ×10<sup>-3</sup></b>	<b>93.7</b>	<b>&lt;10<sup>-6</sup></b>
	<b>SSK71/SPC17</b>	<b>4.3</b>	<b>2.4 ×10<sup>-3</sup></b>	<b>95.7</b>	<b>&lt;10<sup>-6</sup></b>
	<b>SSK71/SPC18</b>	<b>3.7</b>	<b>1.8 ×10<sup>-3</sup></b>	<b>96.3</b>	<b>&lt;10<sup>-6</sup></b>
<b>Pb</b>	<b>SSK71/SPC16</b>	<b>13.9</b>	<b>3.6 ×10<sup>-3</sup></b>	<b>86.1</b>	<b>&lt;10<sup>-6</sup></b>
	<b>SSK71/SPC17</b>	<b>19.8</b>	<b>5.9 ×10<sup>-3</sup></b>	<b>80.2</b>	<b>&lt;10<sup>-6</sup></b>
	<b>SSK71/SPC18</b>	<b>27.0</b>	<b>7.8 ×10<sup>-3</sup></b>	<b>73.0</b>	<b>&lt;10<sup>-6</sup></b>
	<b>SSK80/SPC4</b>	<b>22.7</b>	<b>6.1×10<sup>-3</sup></b>	<b>77.3</b>	<b>&lt;10<sup>-6</sup></b>